Supplementary figures

of the manuscript

Spatial profiling of early primate gastrulation *in utero*

Sophie Bergmann[1,2,3#], Christopher A. Penfold[1,2,3,5#], Erin Slatery[1,2,3#], Dylan Siriwardena[1,2,3], Charis Drummer[6], Stephen Clark[2,4], Stanley E. Strawbridge[1,3], Keiko Kishimoto[7], Alice Vickers[8], Mukul Tewary[8], Timo N. Kohler[9], Florian Hollfelder[9], Wolf Reik[2,4], Erika Sasaki[7], Rüdiger Behr[6] and Thorsten E. Boroviak[1,2,3,*]

1. Department of Physiology, Development and Neuroscience, University of Cambridge, Downing Site, Cambridge CB2 3EG, United Kingdom
2. Centre for Trophoblast Research, University of Cambridge, Downing Site, Cambridge CB2 3EG, United Kingdom
3. Wellcome Trust – Medical Research Council Stem Cell Institute, University of Cambridge, Jeffrey Cheah Biomedical Centre, Puddicombe Way, Cambridge CB2 0AW, United Kingdom
4. Epigenetics Programme, Babraham Institute, Cambridge CB22 3AT, United Kingdom
5. Wellcome Trust – Cancer Research UK Gurdon Institute, Henry Wellcome Building of Cancer and Developmental Biology, University of Cambridge, Tennis Court Road, Cambridge, CB2 1QN, UK
6. Research Platform Degenerative Diseases, German Primate Center, Leibniz-Institute for Primate Research, Kellnerweg 4, 37077 Göttingen, Germany, and DZHK (German Center for Cardiovascular Research), Partner Site Göttingen, 37077 Göttingen, Germany
7. Department of Applied Developmental Biology, Central Institute for Experimental Animals, 3-25-12 Tonomachi, Kawasaki-ku, Kawasaki 210-0821, Japan
8. Centre for Stem Cells and Regenerative Medicine, King's College London, Floor 28, Tower Wing, Guy's Hospital, Great Maze Pond, London SE1 9RT
9. Department of Biochemistry, University of Cambridge, Hopkins Building, Tennis Court Road, Cambridge CB2 1QW, United Kingdom

Content

Supplementary Figure 7 | Diversification of postimplantation hypoblast-derived lineages

Supplementary Figure 8 | 3D in vitro modelling of the marmoset Amnion

Supplementary Figure 9 | Canonical correlation analysis of marmoset, cynomolgus monkey and human pre- and postimplantation embryo datasets.

Supplementary Figure 10 | Cross-species analysis of postimplantation lineages identifies marmoset blood progenitors at CS7.

Supplementary Figure 11 | Cross-species analysis of primate gastrulation *in vivo*

Supplementary Figure 12 | Generation of marmoset naïve pluripotent stem cells

Supplementary Fig. 1

a

Spatial embryo profiling — POST-IMPLANTATION EMBRYO

Carnegie Stage (CS)	Embryonic day	Uterus ID	Embryo ID	Internal structures	Image registration and 3D-reconstruction	No. of cryosections performed (12 µm)	Slide no. with embryo in cavity	No. of embryo slides	Embryo size (µm)	Immuno-fluorescence	LCM for Smart-Seq2	No. of Smart-Seq2 samples sequenced	No. of Smart-Seq2 samples after QC
CS5	E14-16	U15A	E15A	partially broken	no	200	n.a.	1	n.a.	yes	yes	24	20
CS5	E14-16	U15B	E15B	intact	yes	220	188 - 215	27	324	yes	yes	284	237
CS6	E14-16	U15C	E15Cb	intact	yes	265	200 - 227	27	348	yes	yes	272	200
CS6	E14-16	U15C	E15Ca	intact	yes	265	229 - 262	33	420	yes	yes	444	348
CS7	E24-26	U25A	E25A	intact	yes	202	131 - 202	71	1488	yes	yes	302	265
CS7	E24-26	U25B	E25B	partially broken	no	210	118 - 190	72	1236	yes	yes	146	136
CS7	E24-26	U25D	E25D	partially broken	no	305	131 - 257	126	1536	yes	yes	440	358
TOTAL												1,912	1,564

b

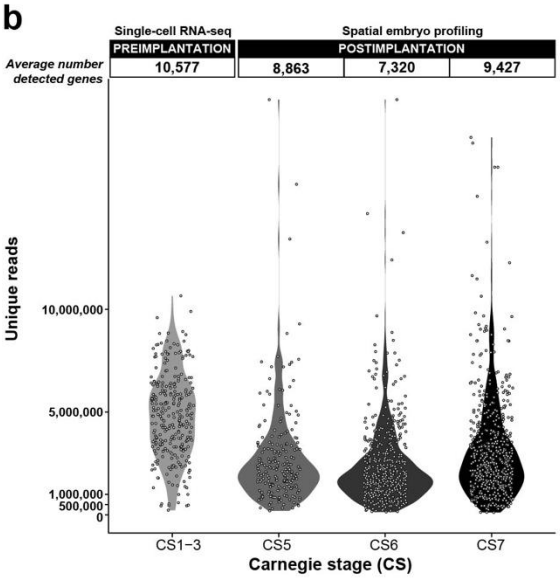

c

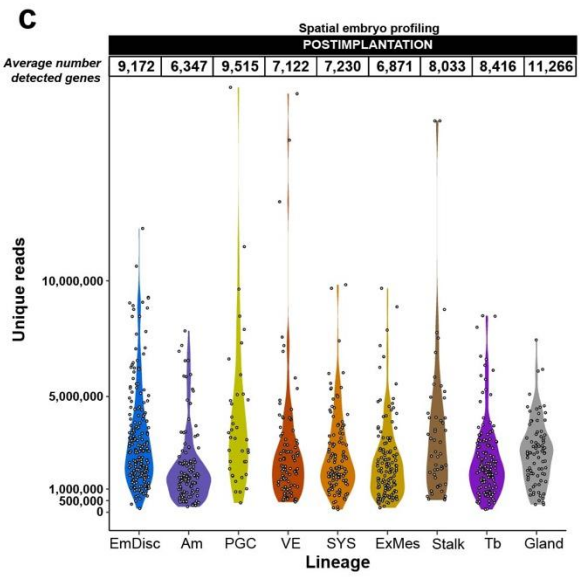

d

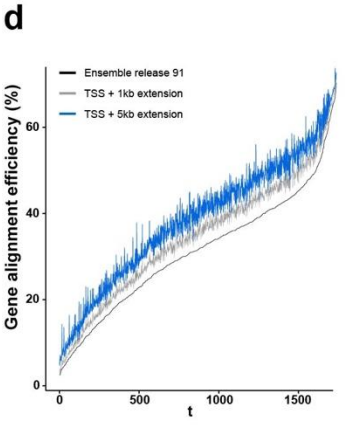

e

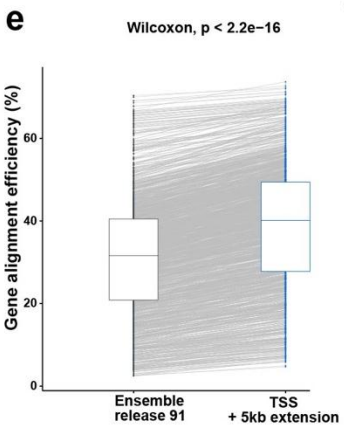

f

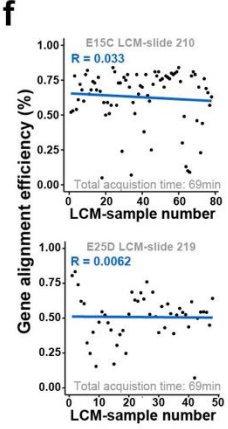

g

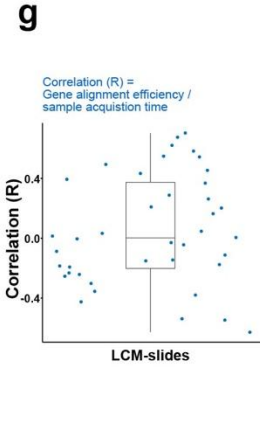

h

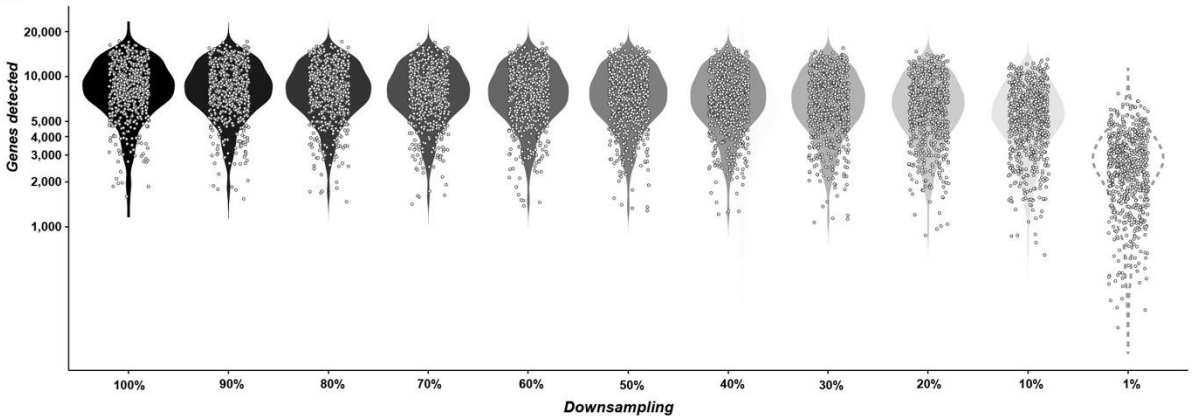

Supplementary Figure 1 | Spatial embryo profiling generates high-quality transcriptomes

a, Summary of postimplantation embryos processed for spatial embryo profiling. Number of samples obtained by spatial embryo profiling of each stage are indicated along with numbers passing quality control used for downstream analysis (n=841 samples).

b, Unique reads of spatial embryo profiling for postimplantation stages show comparable sequencing depth to preimplantation marmoset single-cell sequencing data published in Boroviak et al. (2018), with an average 2 million reads per sample.

c, Unique reads of postimplantation embryo lineages and maternal glands processed by spatial embryo profiling show consistent average read numbers across tissue types. . EmDisc, Embryonic disc; Am, Amnion; SYS, Secondary Yolk Sac; VE, Visceral Endoderm; Tb, Trophoblast; ExMes, Extraembryonic mesoderm; PGCs, Primordial Germ Cells; Gland, Maternal endometrial glands.

d, Gene alignment efficiency for spatial embryo profiling. For downstream analysis, genes were aligned to a modified gtf file based on marmoset Ensembl release 91 with TSS extended by 5kb. Alignment efficiency using the modified gtf file was higher than for the standard Ensembl release 91 and when extending TSS by 1kb for all samples. Individual samples are ordered by alignment efficiency. TSS, Transcription stop site.

e, Mean mapping efficiency using the extended gtf file was statistically significantly greater than using the standard Ensemble release 91 based upon a paired Wilcoxon test.

f, Influence of sample acquisition time on gene alignment efficiency. The gene alignment efficiency of the individual LCM samples is correlated with the order of sample acquisition. Spearman's correlation coefficient was used to gauge the impact of sample acquisition time with sample quality. Here, we additionally fit a linear model on two representative plots from different developmental stages (CS5 and CS7). No significant correlation is observed.

g, Correlation analysis of gene alignment efficiency by sample acquisition time. Spearman's correlation coefficient between gene alignment efficiency and sample acquisition time for processed embryo sections did not show a significant deviation from 0.

h, Number of unique genes detected per sample. On average >8,000 genes were detected per LCM sample. We simulated the effect of shallower sequencing on gene detection by down sampling the count matrix using the downsampleMatrix function from DropletUtils. This indicated that we retained a high number of unique genes following stringent down sampling.

Supplementary Fig. 2

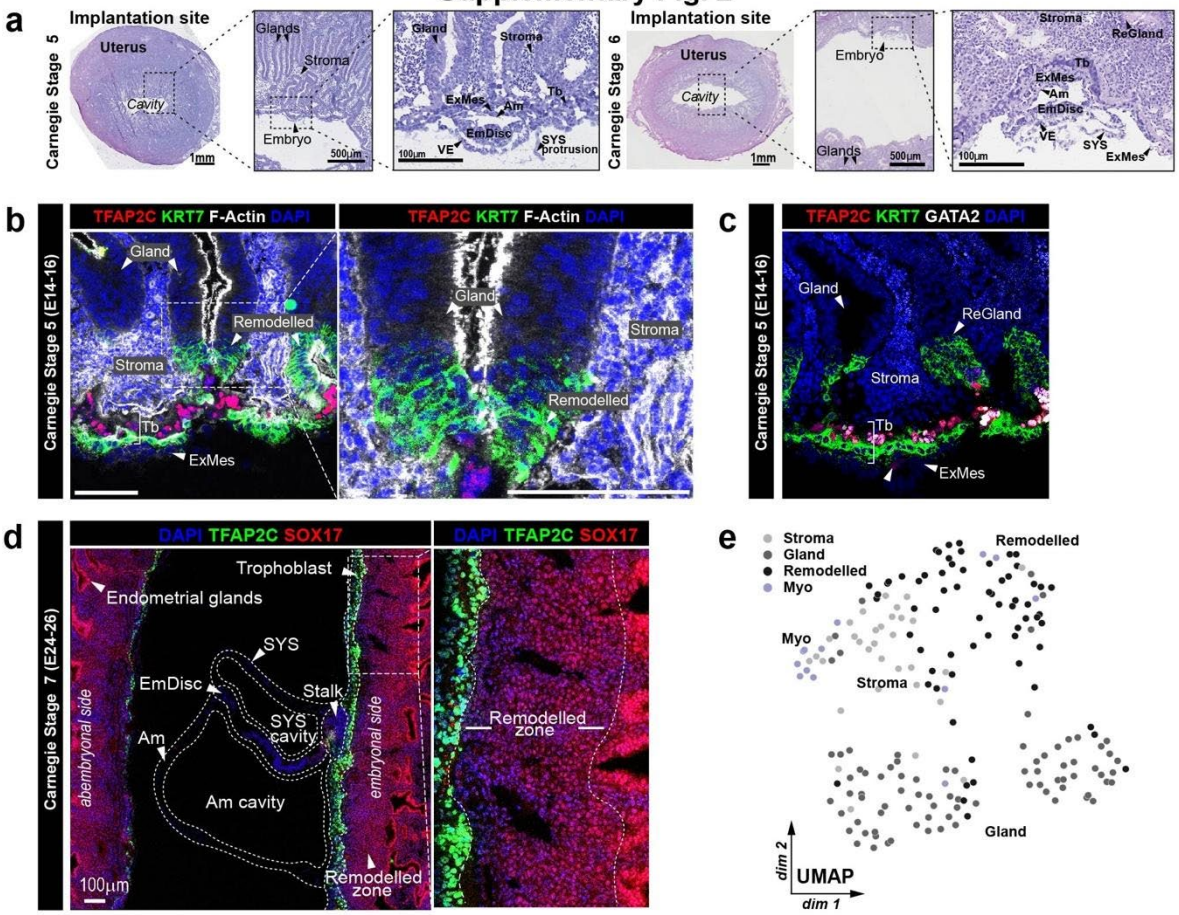

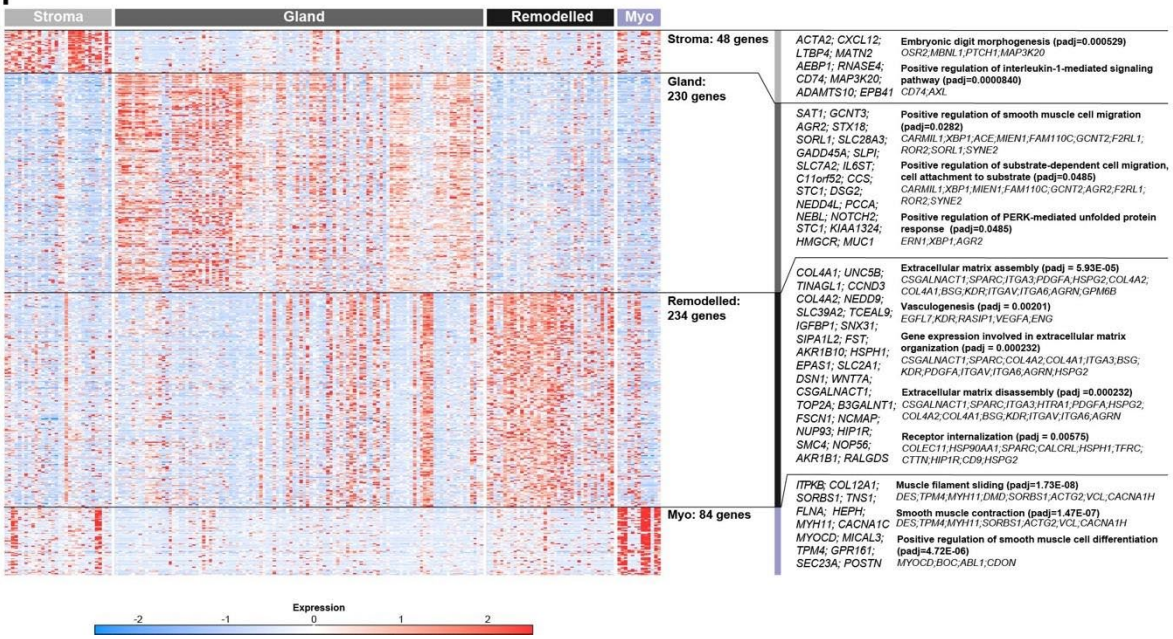

Supplementary Figure 2 | STEP analysis of the pregnant uterus

a, Implantation sites of CS5 and CS6 embryos stained by haematoxylin and eosin (H&E). Uterus cross-section on the left, zoom-ins show embryo implantation site (middle) and annotated embryo in greater detail (right). EmDisc, Embryonic Disc; SYS, Secondary Yolk Sac; VE, Visceral Endoderm; ExMes, Extraembryonic Mesoderm; Am, Amnion; Tb, Trophoblast; ReGland, Remodelled gland.

b-d, Immunofluorescence image of implantation site at CS5 (b-c) and CS7 (d)**.** Inset at CS5 highlights remodelled endometrial gland undergoing epithelial plaque reaction, positive for KRT7. Inset at CS7 highlights loss of nuclear SOX17 in endometrial glands in the remodelled zone of the endometrium. Scale bars represent 100 μm. Am: Amnion; ExMes: Extraembryonic Mesoderm; ReGland: Remodelled endometrial gland; Tb: Trophoblast.

e, UMAP of maternal stroma, gland, remodelled endometrium, and myometrium based on the whole transcriptome (20,000 genes). UMAP: Uniform Manifold Approximation and Projection for Dimension Reduction.

f, Heatmap of expression of differentially expressed genes (DEG) in maternal lineages displayed in (e). Representative genes (left) and key gene ontology (GO) enrichment analysis (right) are shown. Genes shown in heatmap from Seurat function *FindAllMarkers* (minimum percent 50%, minimum log fold change 0.25) and filtered by adjusted p-value <0.05.

Supplementary Fig. 3

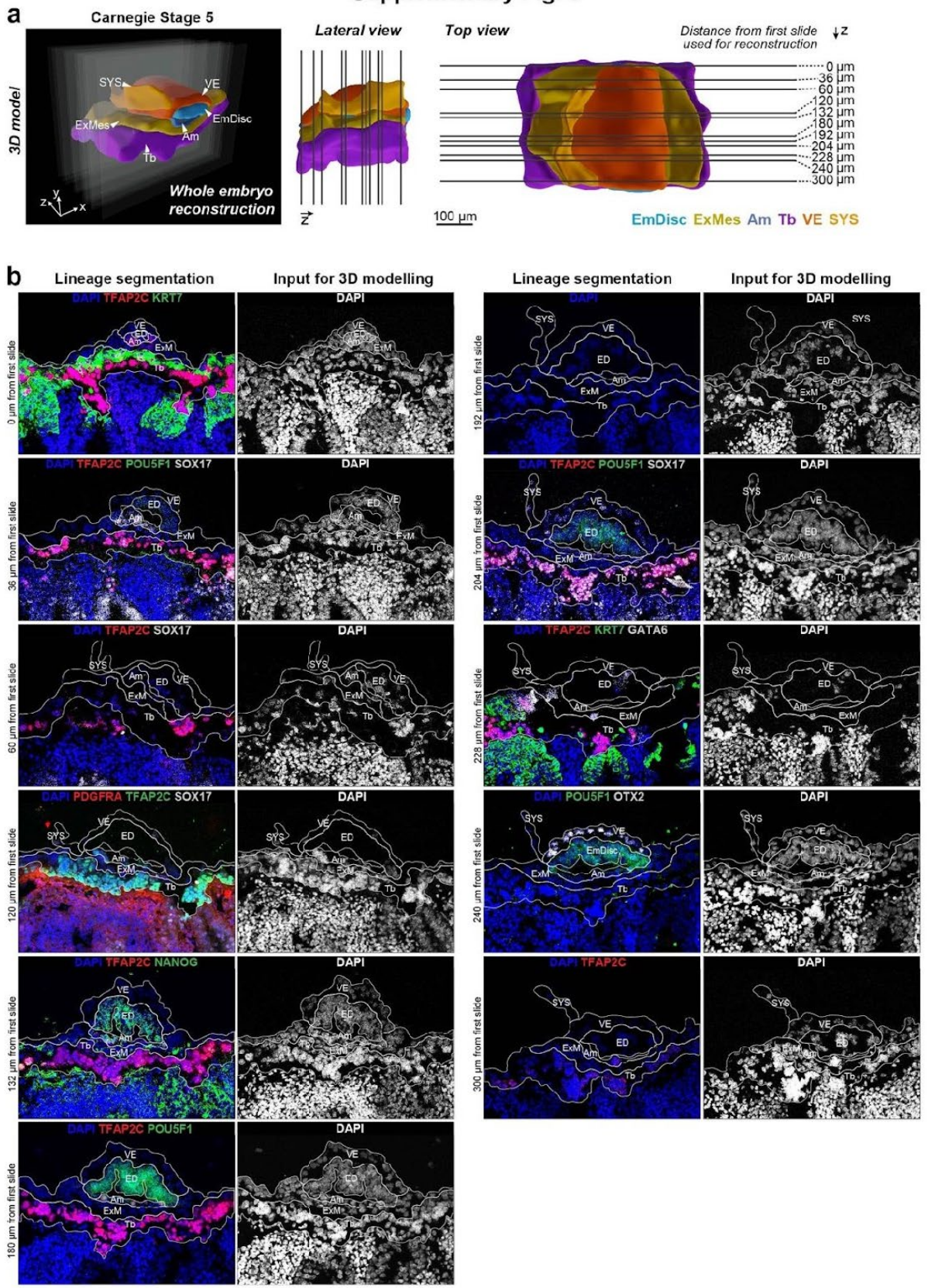

Supplementary Figure 3 | Virtual reconstruction of the Carnegie stage 5.

a, Virtual 3D reconstruction of the Carnegie stage 5 embryo viewed from front, side (lateral view) and above (top view). Embryo sections processed for 3D-reconstructions shown in all views as lines. Distance from first slide used for reconstruction indicated on the right of panel.

b, Representative immunofluorescence sections used for the embryo model shown in a. White lines outline the areas that were segmented based on lineage-specific markers, morphology and tissue location. TFAP2C and KRT7 for Tb, SOX17 for SYS, maternal endometrial glands and PGCs (together with TFAP2C), POU5F1 and NANOG for EmDisc, OTX2 and GATA6 for VE, TFAP2C for Am, PDGFRA for ExMes and based on morphology and location. Relative position of consecutive slides in relation to first slide used for reconstruction indicated on left side. Slides used for LCM-sample acquisition prior to immunofluorescence staining indicated bottom left as 'LCM slide'. DAPI used for nuclei labelling.

EmDisc/ED, Embryonic Disc; SYS, Secondary Yolk Sac; VE, Visceral Endoderm; ExMes/ExM, Extraembryonic Mesoderm; Am, Amnion; Tb, Trophoblast.

Supplementary Fig. 4

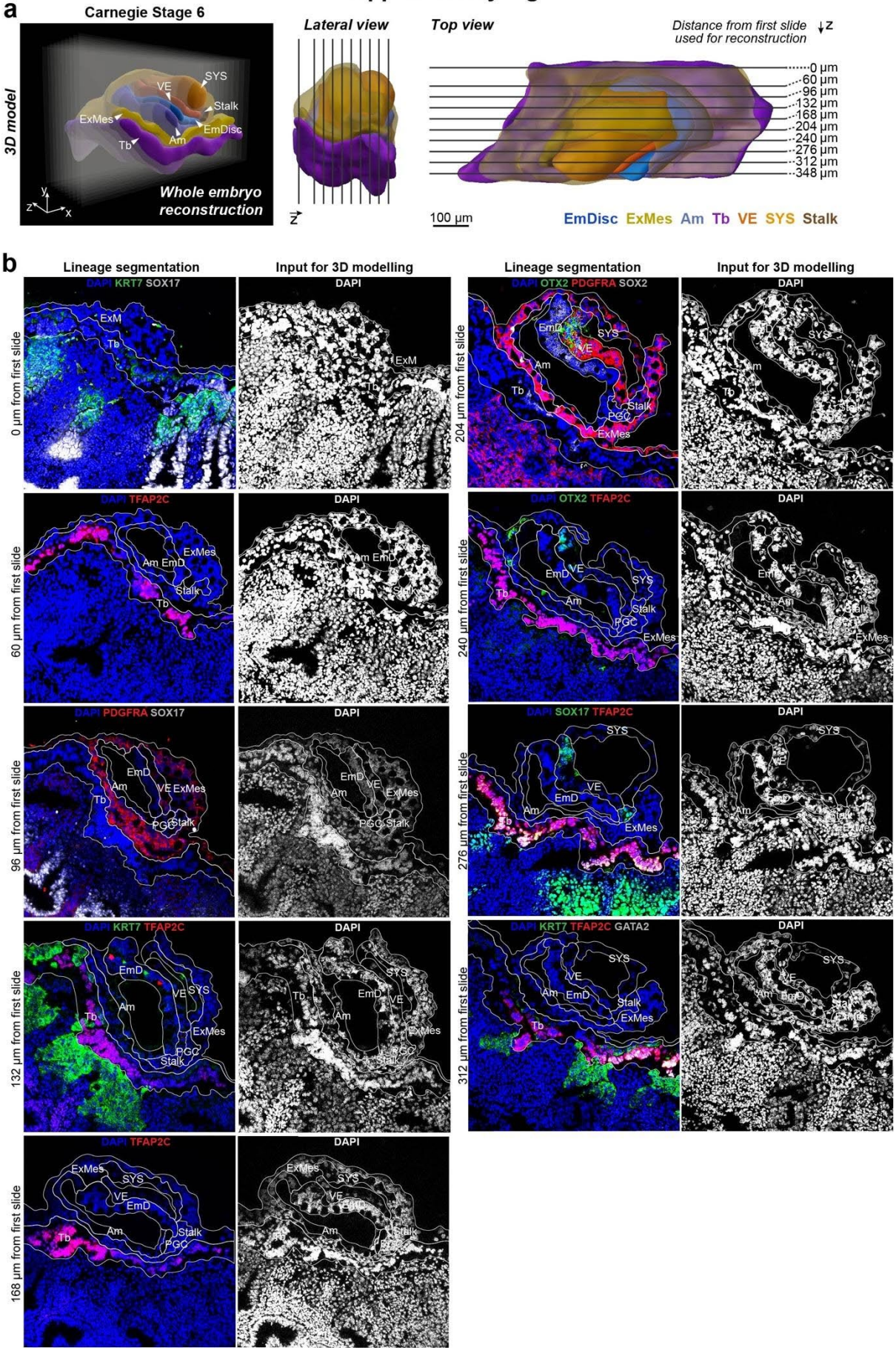

Supplementary Figure 4 | Virtual reconstruction of Carnegie stage 6.

a, Virtual 3D reconstruction of a Carnegie stage 6 embryo viewed from front, side (lateral view) and above (top view). Embryo sections processed for 3D-reconstructions shown in all views as lines. Distance from first slide used for reconstruction indicated on the right of panel.

b, Representative immunofluorescence sections used for the embryo model shown in a. White lines outline the areas that were segmented based on lineage-specific markers, morphology and tissue location. TFAP2C, KRT7 and GATA2 labelled Tb, PDGFRA marked VE, SYS and ExMes, SOX2 labelled EmDisc, SOX17 and OTX2 marked VE. Am and ExMes were traced based on morphology and location. Relative position of consecutive slides in relation to first slide used for reconstruction indicated on left side. All slides were used for LCM processing prior to staining. DAPI used for nuclei labelling.

EmDisc/ED, Embryonic Disc; SYS, Secondary Yolk Sac; VE, Visceral Endoderm; ExMes/ExM, Extraembryonic Mesoderm; Am, Amnion; Tb, Trophoblast.

Supplementary Fig. 5

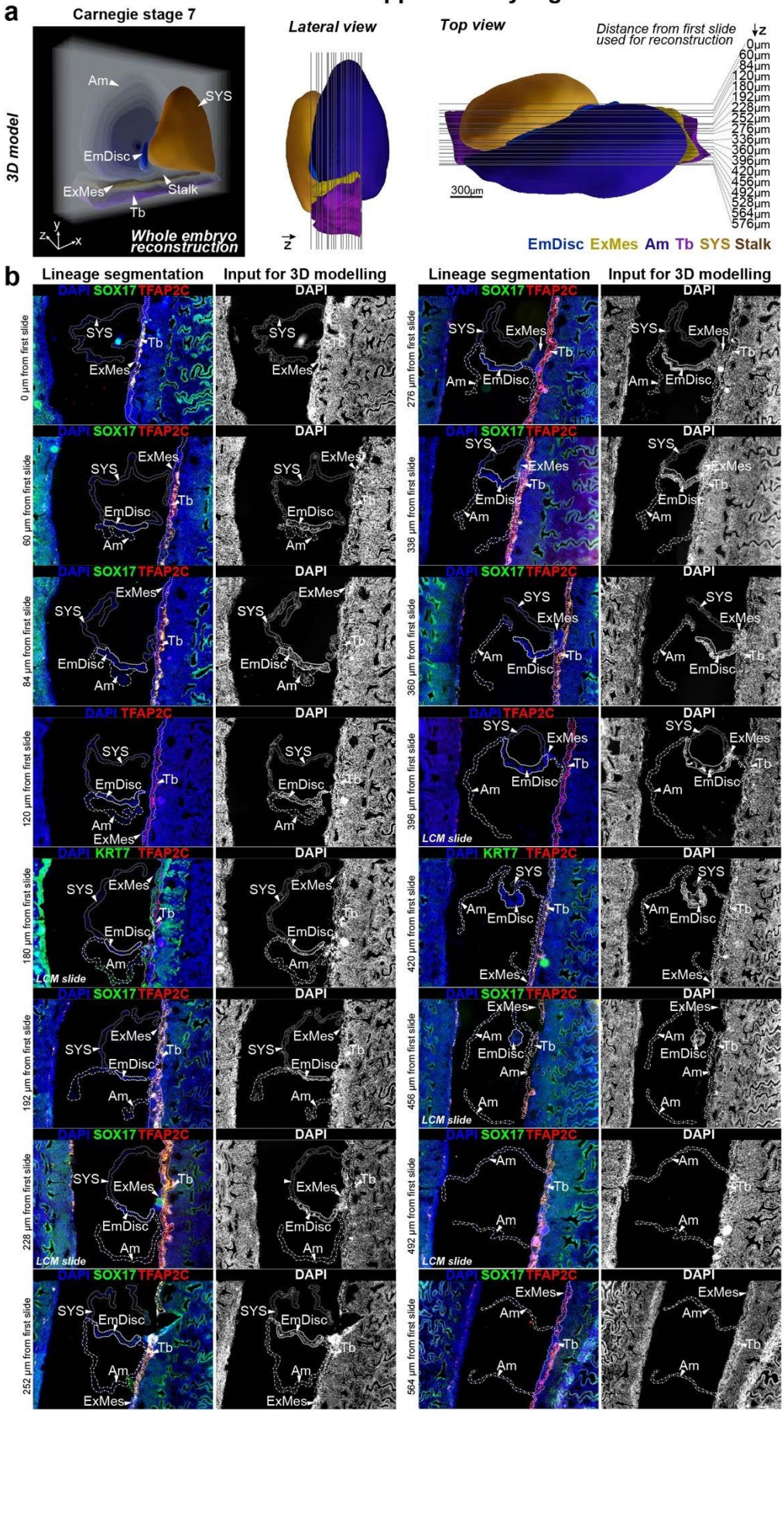

Supplementary Figure 5 | Virtual reconstruction of Carnegie stage 7.

a, Virtual 3D reconstruction of a Carnegie stage 7 embryo viewed from front, side (lateral view) and above (top view). Embryo sections processed for 3D-reconstructions shown in all views as lines. Distance from first slide used for reconstruction indicated on the right of panel

b, Representative immunofluorescence sections used for the embryo model shown in a. White lines outline the areas that were segmented based on lineage-specific markers, morphology and tissue location. TFAP2C and KRT7 labelled Tb, KRT7 marked for Am, SOX17 marked maternal glands. EmDisc, SYS and ExMes were traced based on morphology and location. Relative position of consecutive slides in relation to first slide used for reconstruction indicated on left. Slides used for LCM processing prior to staining indicated bottom left as 'LCM slide'. DAPI used for nuclei labelling.

EmDisc, Embryonic Disc; SYS, Secondary Yolk Sac; VE, Visceral Endoderm; ExMes, Extraembryonic Mesoderm; Am, Amnion; Tb, Trophoblast.

Supplementary Fig. 6

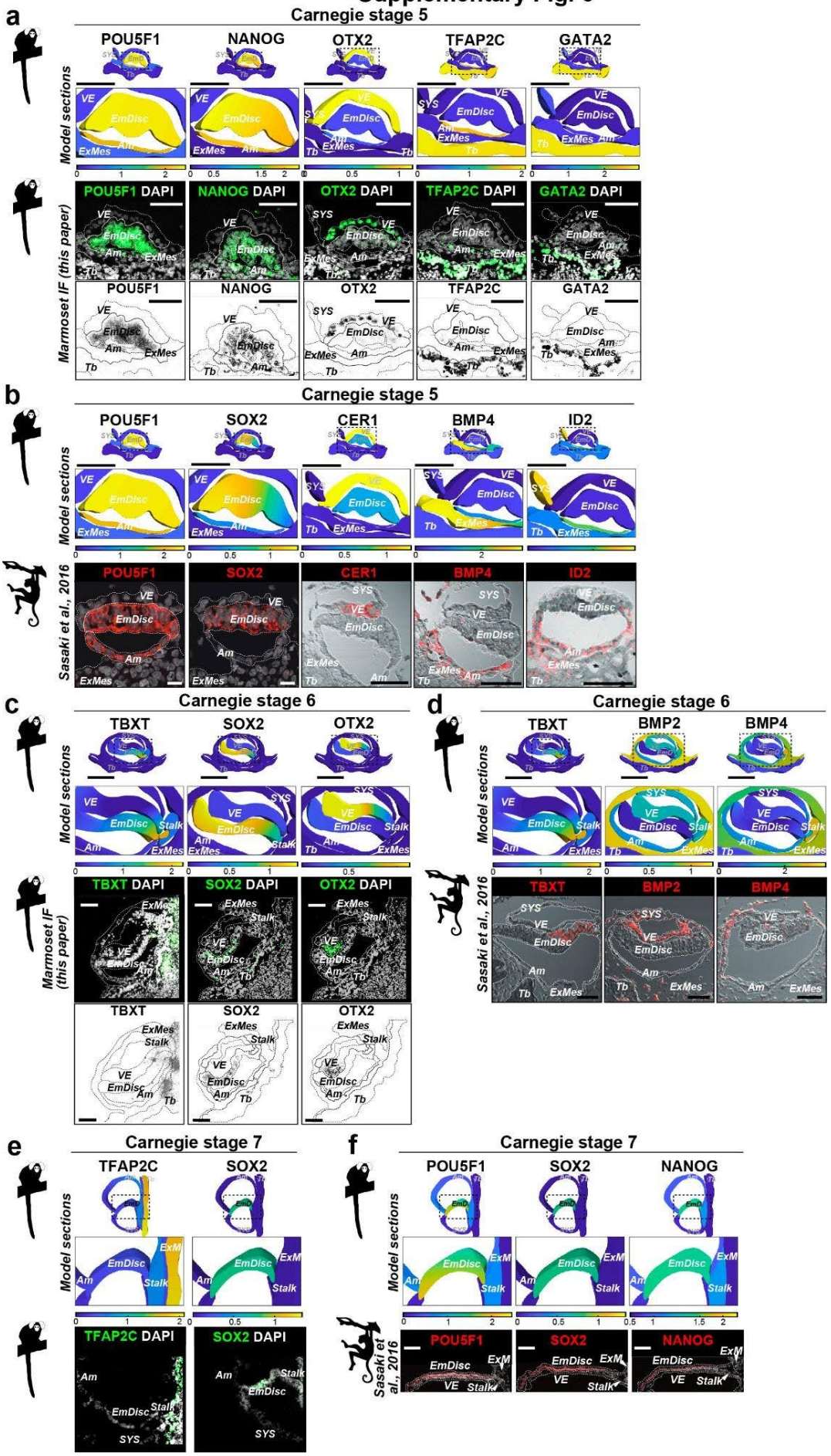

Supplementary Figure 6 | Marmoset 3D-transcriptomes recapitulate marmoset immunostaining and cynomolgus expression patterns

a, Comparison of marmoset 3D-transcriptome models to immunostainings at CS5. Cross sections displaying lineage-specific gene expression compared to immunostainings of the matched marmoset embryo overlaid with DAPI (top) or as inverted single-channel image (bottom). Scale bars represent 100 µm.

b, Comparison of marmoset 3D-transcriptome models to cynomolgus at CS5. Cross sections displaying lineage-specific gene expression compared to *in situ* hybridisations of stage matched cynomolgus monkey embryos. Source of embryo images of postimplantation embryos indicated next to individual images. Scale bars represent 100 µm.

c, Comparison of marmoset 3D-transcriptome models to immunostainings at CS6.

Cross sections displaying lineage-specific gene expression compared to immunostainings of the matched marmoset embryo overlaid with DAPI (top) or as inverted single-channel image (bottom). Scale bars represent 100 µm.

d, Comparison of marmoset 3D-transcriptome models to cynomolgus at CS6.

Cross sections displaying lineage-specific gene expression compared to *in situ* hybridisations of stage-matched cynomolgus monkey embryos. Source of embryo images of postimplantation embryos indicated next to individual images. Scale bars represent 100 µm.

e, Comparison of marmoset 3D-transcriptome models to immunostainings at CS7.

Cross sections displaying lineage-specific gene expression compared to immunostainings of the matched marmoset embryo overlaid with DAPI (top). Scale bars represent 100 µm.

f, Comparison of marmoset 3D-transcriptome models to cynomolgus at CS7.

Cross sections displaying lineage-specific gene expression compared to *in situ* hybridisations of stage-matched cynomolgus monkey embryos. Source of embryo images of postimplantation embryos indicated next to individual images. Scale bars represent 100 µm.

Supplementary Fig. 7

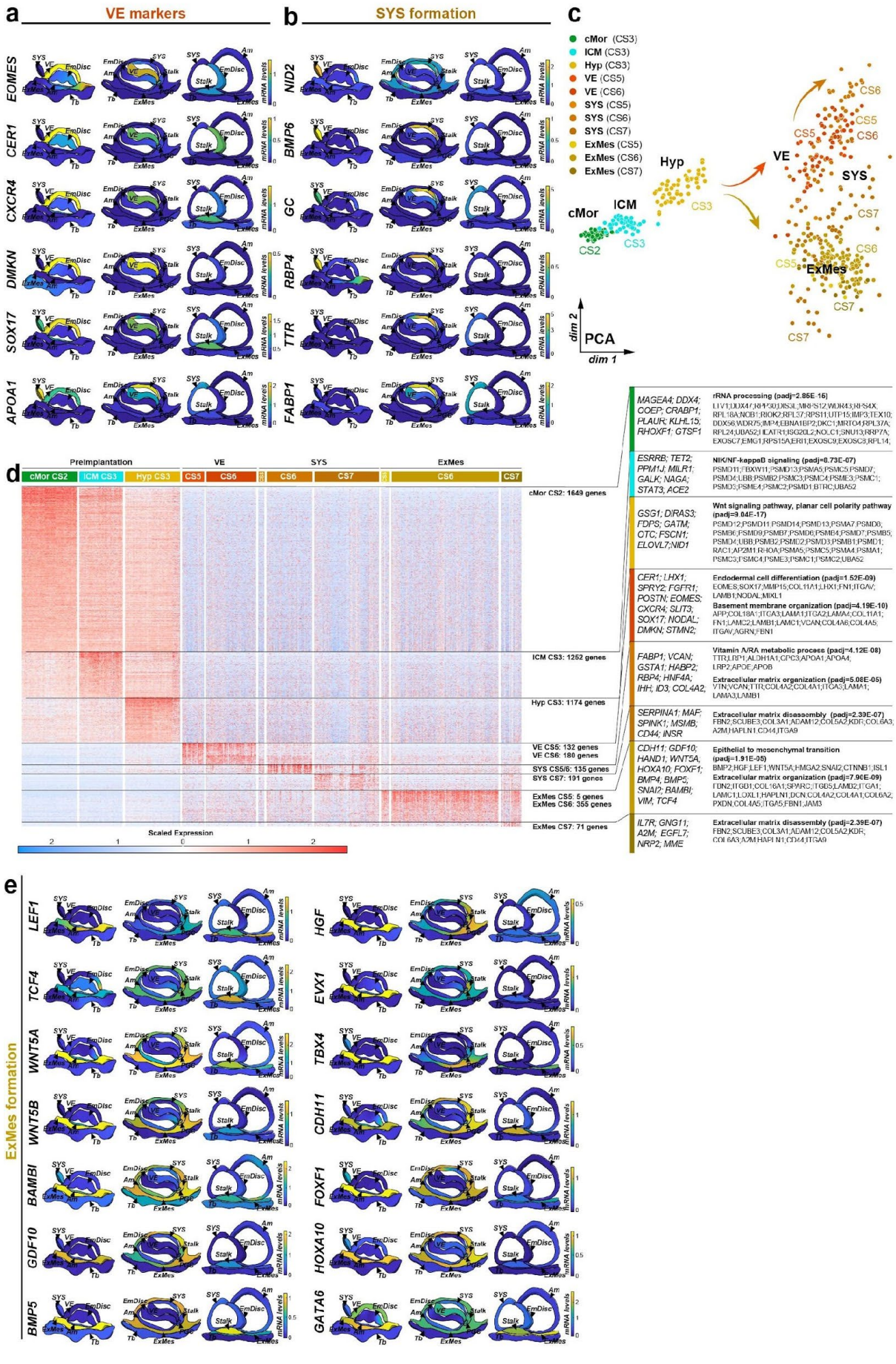

Supplementary Figure 7 | Diversification of postimplantation hypoblast-derived lineages

a, b Virtual cross-sections of 3D-transcriptomes at CS5, 6 and 7 for (a) VE-associated transcripts and (b) SYS formation.

c, PCA of hypoblast and related lineages, based on the top 5000 most variable genes, PC1=18.7%, PC2=13.2%.

d, Heatmap of expression of differentially expressed genes (DEG) in extraembryonic lineages displayed in (c). Representative genes (left) and key gene ontology (GO) enrichment analysis (right) are shown. Genes shown in heatmap from Seurat function *FindAllMarkers* (minimum percent 50%, minimum log fold change 0.25) and filtered by adjusted p-value <0.05.

e, Virtual cross-sections of 3D-transcriptomes at CS5, 6 and 7 depicting markers and expression gradients for ExMes.

cMor, compacted morula; ICM, inner cell mass; Hyp, hypoblast; SYS, Secondary Yolk Sac; VE, Visceral Endoderm; ExMes, Extraembryonic Mesoderm; EmDisc, Embryonic Disc; Am, Amnion; Tb, Trophoblast.

Supplementary Fig. 8

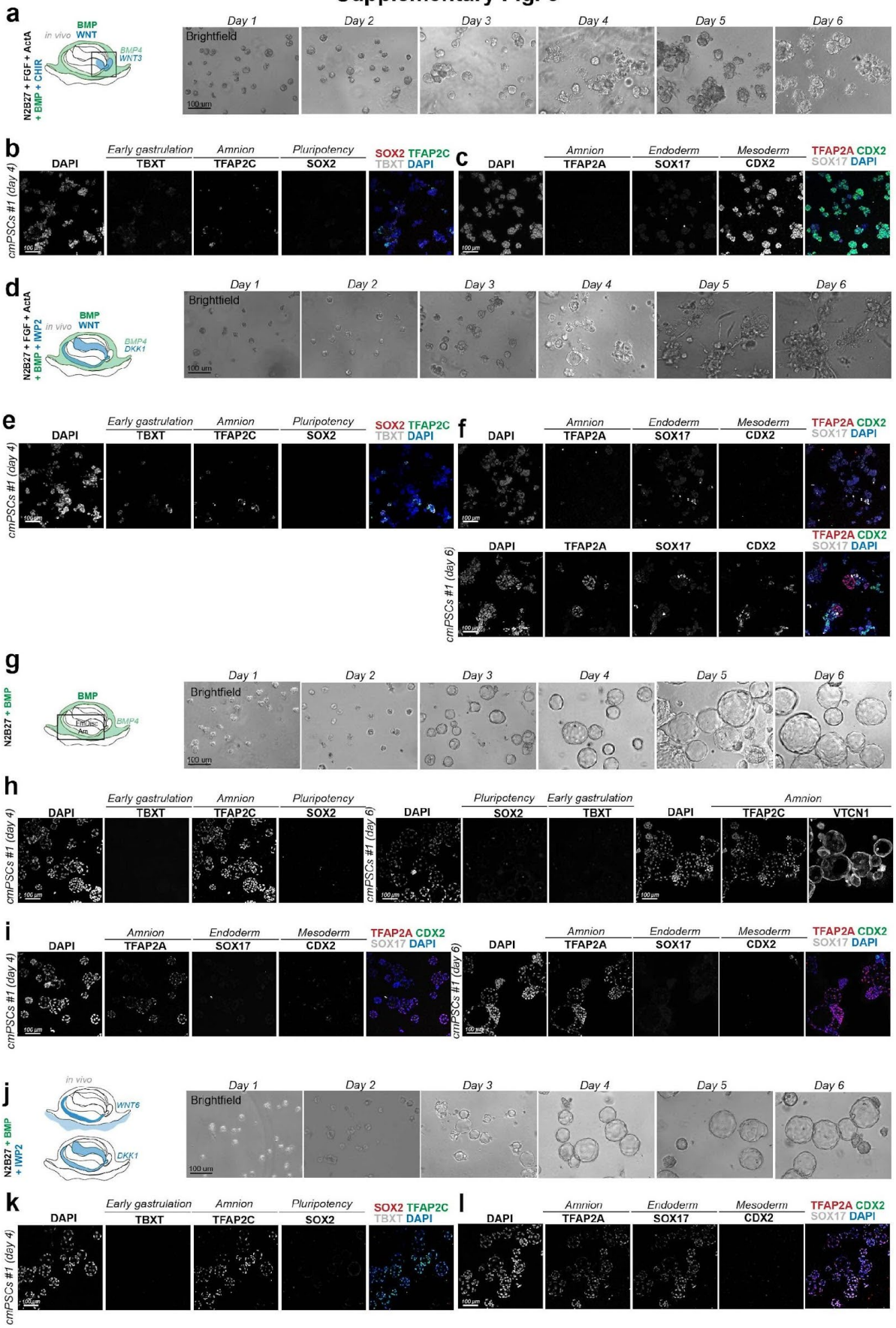

Supplementary Figure 8 | 3D in vitro modelling of the marmoset Amnion

a, Overlay schematic of WNT and BMP signalling in the marmoset embryo. The ExMes, amnion, and PGCs are sources of *BMP4* in the embryo and the posterior EmDisc, stalk and PGCs express *WNT3*. mRNA expression gradients summarised in CS6 cross section (left). Time series brightfield images of interphase culture with FGF and Activin A + CHIR + BMP4 (right)**.** Structures formed irregularly shaped cell clusters at day 3 and continue to expand to day 6.

b-c, Molecular characterisation of BMP- and WNT-treated EmDisc model structures at day 4. Representative maximum projection images from immunostaining at day 4 from staining for pluripotency (SOX2), early gastrulation (TBXT), amnion (TFAP2C, TFAP2A), endoderm (SOX17) or mesoderm (CDX2) markers. Structures exhibited loss of SOX2 expression and homogenous expression of CDX2, but low/absent expression of TFAP2C, TFAP2A or SOX17, consistent with mesodermal fate.

d, Overlay schematic of WNT inhibition and BMP signalling in the marmoset embryo. The ExMes, amnion, and PGCs are sources of *BMP4* in the embryo and the VE and Amnion express canonical WNT inhibitor *DKK1*. mRNA expression gradients summarised in CS6 cross section (left). Time series brightfield images of interphase culture with FGF and Activin A + IWP-2 + BMP4 (right)**.** The emergence of disorganized, differentiated populations was evident at day 4.

e-f, Molecular characterisation of BMP-treated and WNT-inhibited EmDisc model structures at day 4. Representative maximum projection images from immunostaining at day 4 (top panel) or day 6 (bottom panel) from staining for pluripotency (SOX2), early gastrulation (TBXT), amnion (TFAP2C, TFAP2A), endoderm (SOX17) or mesoderm (CDX2) markers. By day 4, structures lost SOX2 expression, indicating loss of pluripotency. By day 6, structures upregulated TFAP2A, SOX17, and CDX2.

g, Overview schematic of BMP signalling in the marmoset embryo. The ExMes, amnion, and PGCs are sources of *BMP4* in the embryo. mRNA expression gradients summarised in CS6 cross section (left). Time series brightfield images of interphase culture with BMP4 produces amnion-like structures (right). Structures formed homogenous squamous epithelial cysts, reminiscent of the amnion. Structures first open a lumen at day 3 and expand up to day 6.

h-i, Molecular characterisation of Amnion-like structures at day 4. Representative maximum projection images from immunostaining at day 4 (left panel) or day 6 (right panel) from staining for pluripotency (SOX2), early gastrulation (TBXT), amnion (TFAP2C, TFAP2A,

VTCN1), Amnion/ExMes (ISL1), endoderm (SOX17) or mesoderm (CDX2) markers. TFAP2C was upregulated by day 4, and TFAP2A and VTCN1 were highly expressed by day 6, indicative of a mature amnion fate (also see Fig. 1f). Structures were negative for SOX2, SOX17, and CDX2.

j, Overlay schematic of WNT inhibition and WNT6 expression in the marmoset embryo. The VE and amnion express canonical WNT inhibitor *DKK1*, and the amnion expresses WNT family member *WNT6*. mRNA expression gradients summarised in CS6 cross section (left). Time series brightfield images of interface culture with IWP-2 + BMP4 (right). Similar to BMP alone, structures formed homogenous squamous epithelial cysts, reminiscent of the amnion. Structures first open a lumen at day 3 and expand up to day 6.

k, l, Molecular characterisation of BMP-treated and WNT-inhibited Amnion-like structures at day 4. Representative maximum projection images from immunostaining at day 4 from staining for pluripotency (SOX2), early gastrulation (TBXT), amnion (TFAP2C, TFAP2A), endoderm (SOX17) or mesoderm (CDX2) markers. Scale bars represent 100 μm. Structures upregulated both TFAP2A and TFAP2C by day 4, and retained expression of SOX17, consistent with an early amnion fate.

Supplementary Fig. 9

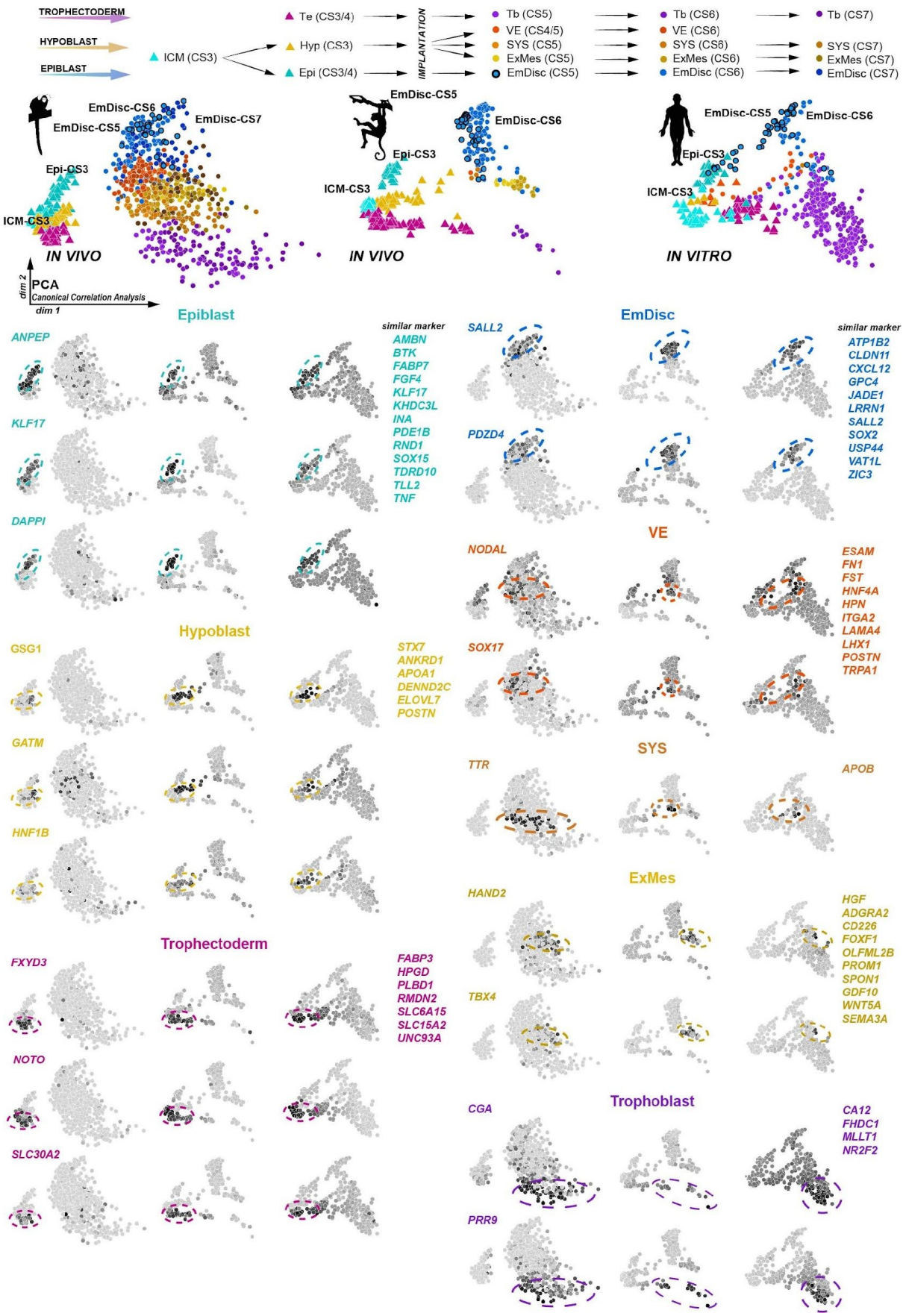

Supplementary Figure 9 | Canonical correlation analysis of marmoset, cynomolgus monkey and human pre- and postimplantation embryo datasets.

Embryo *in vivo* and *in vitro* datasets of pre- to postimplantation cynomolgus monkey[25], *in vitro*-cultured human[12], preimplantation marmoset (ref[24] and this study), and postimplantation marmoset embryo data (this study) were aligned. An overview of the blastocyst lineages and their derivatives during developmental progression is shown on the top of the panel. The colour code for the lineage types is indicated in the schematic overview panel in Fig 1c(preimplantation stages=green/turquoise, embryonic lineage and derivatives=blue, hypoblast-derived lineages=yellow, trophoblast-derived lineages=purple). Visualisation of aligned datasets by PCA shows separation of preimplantation (on the left) and postimplantation (on the right) samples conserved in all species and similar lineage segregation events between primates.

CS5 EmDisc samples are highlighted by a bold black circle, highlighting interclustering of human CS5 EmDisc and CS3 Epiblast samples. *In vitro*-cultured human embryos showed slower segregation kinetics, including delayed EmDisc development and intermixing of ICM and Te samples.

Evolutionarily conserved high-confidence markers expressed in preimplantation (left column) and postimplantation (right column) lineages are plotted on aligned PCA according to named lineage. For each lineage, characteristic marker genes are shown, with genes exhibiting similar patterns listed on the right side.

PCA, Principal component analysis; ICM, Inner cell mass; Epi, Epiblast; Hyp, Hypoblast; Te, Trophectoderm; EmDisc, Embryonic disc; VE, Visceral endoderm; ExMes, Extraembryonic Mesoderm; SYS, Secondary Yolk Sac; Tb, Trophoblast; PGCs, Primordial Germ Cells.

Supplementary Fig. 10

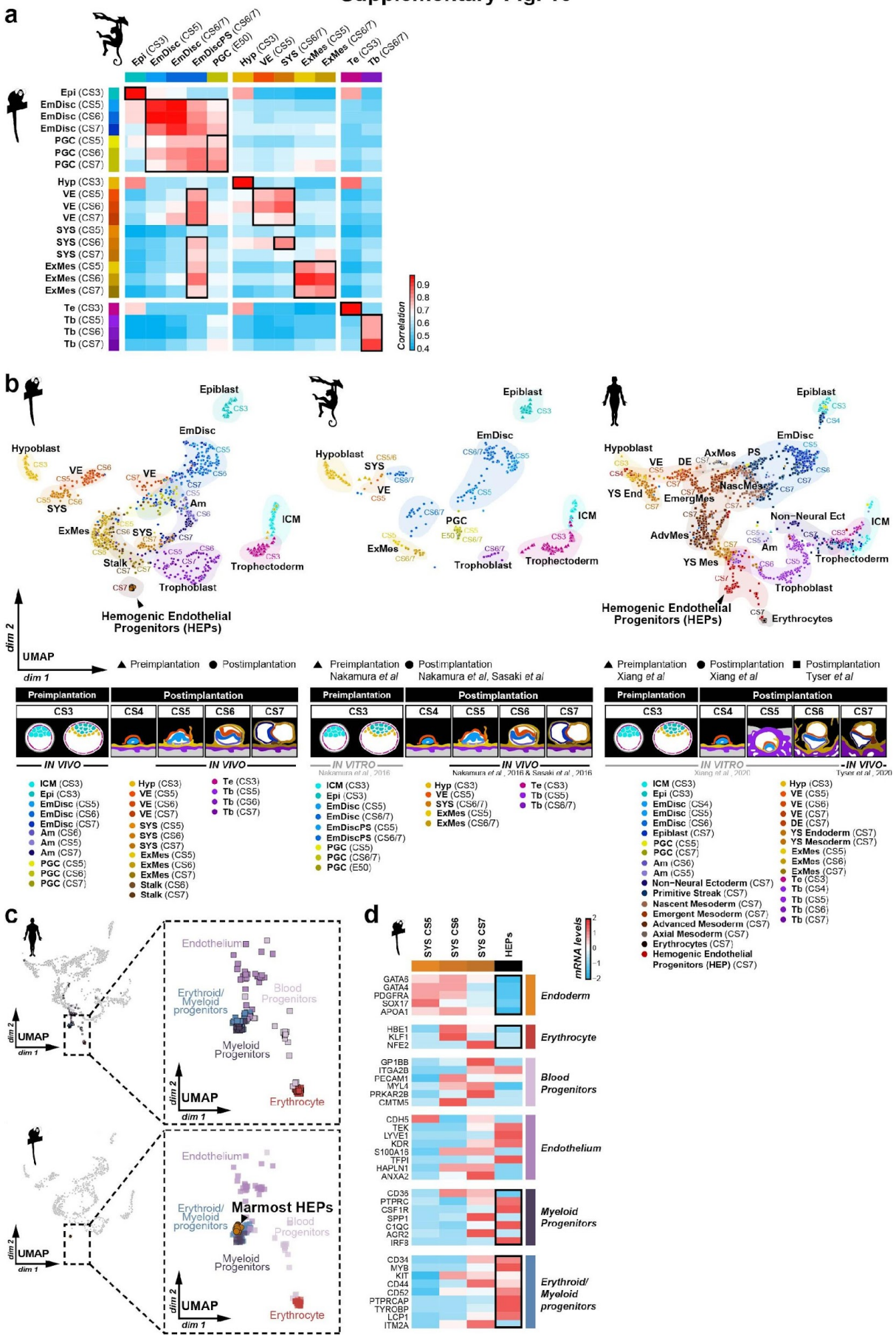

Supplementary Figure 10 | Cross-species analysis of postimplantation lineages identifies marmoset blood progenitors at CS7.

a, Correlation between marmoset and cynomolgus postimplantation lineages. Embryo *in vivo* and *in vitro* datasets of pre- to postimplantation cynomolgus monkey[1], preimplantation marmoset (ref[3] and this study), and postimplantation marmoset embryo data (this study) were compared by Pearson's correlation. Gast1, Gast2a, and Gast2b populations were combined as "EmDiscPS" for alignment to other species.

b, Alignment of marmoset, cynomolgus macaque, and human postimplantation datasets. Embryo *in vivo* and *in vitro* datasets of pre- to postimplantation cynomolgus monkey[1], *in vitro*-cultured human[2], *in vivo* human CS7[43], preimplantation marmoset (ref[3] and this study), and postimplantation marmoset embryo data (this study) were aligned.

Visualisation of aligned datasets by uniform manifold approximation and projection for dimension reduction (UMAP) shows cross-species clustering of pre- and postimplantation lineages, and a subcluster of marmoset SYS samples that align with human CS7 hemogenic endothelial progenitors.

c, UMAP inset highlights blood progenitor subtypes annotated in ref[43]. Inset from human (top panel) and marmoset (bottom panel) UMAP in (b) recoloured to annotate endothelium, erythroid/myeloid progenitors, myeloid progenitors, and erythrocytes shows marmoset cluster aligns specifically to erythroid/myeloid and myeloid progenitors.

d, Heatmap of SYS and blood progenitor markers in marmoset samples. Relative mRNA levels were centred and scaled across samples; SYS, Secondary Yolk Sac; HEP, Hemogenic endothelial progenitors.

Supplementary Fig. 11

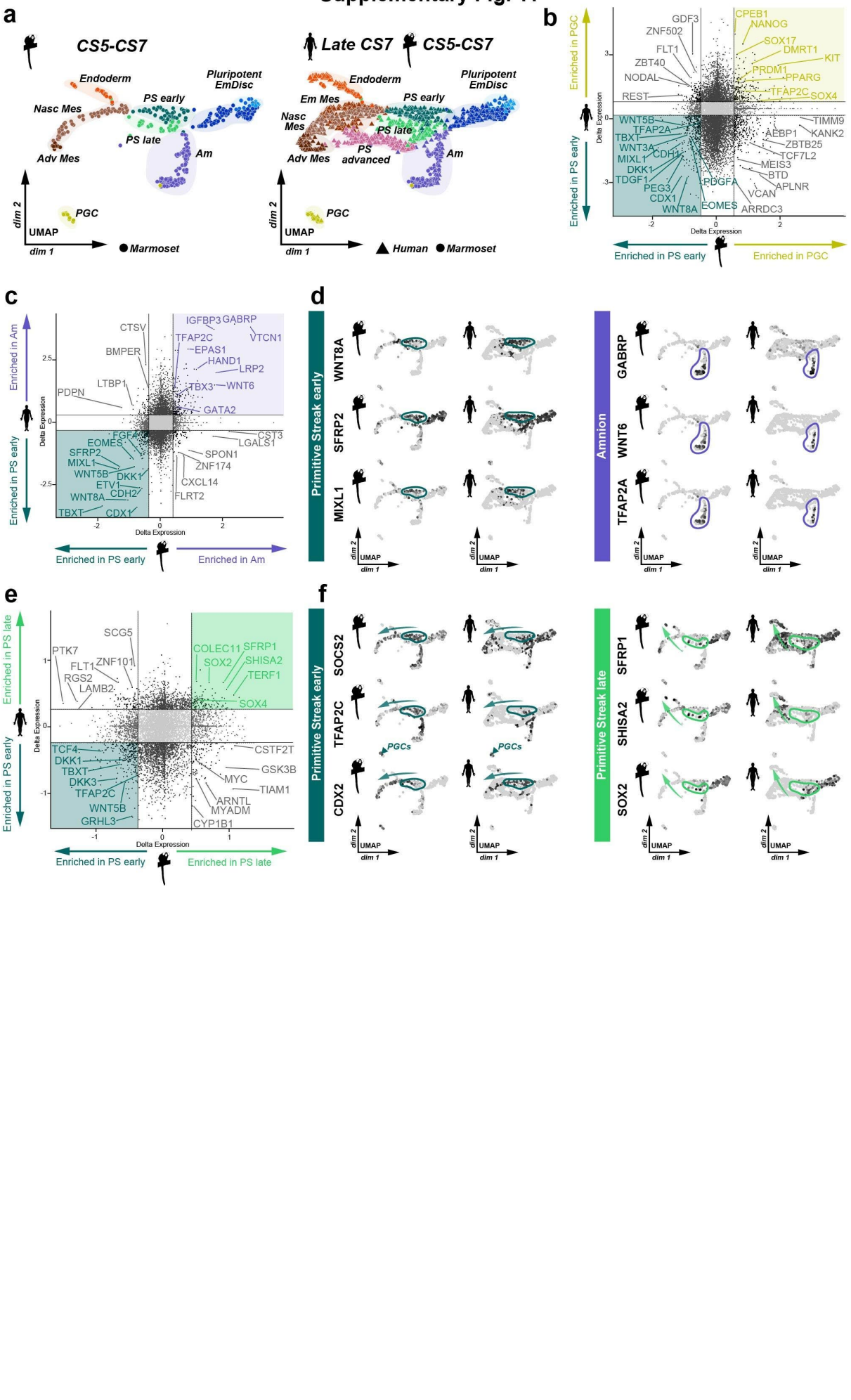

Supplementary Figure 11 | Cross-species analysis of primate gastrulation *in vivo*

a, Unbiased clustering of gastrulation stage lineages represented in UMAP in Extended Data Fig. 19a resolves 9 clusters by shared nearest neighbour clustering**:** Pluripotent EmDisc (Embryonic Disc), PS early (Primitive Streak early), PS late (Primitive Streak late), PS advanced (Primitive Streak advanced), Endoderm, Nasc Mes (Nascent Mesoderm), Em Mes (Emergent Mesoderm), Adv Mes (Advanced Mesoderm), PGCs (Primordial Germ Cells). Reprinted from Extended Data Fig 19c.

b, Human vs. marmoset scatterplots of PGC (primordial germ cell) vs. PS early (primitive streak early). Highlighted quadrants show human-marmoset conserved markers for each lineage, whereas white quadrants show species-specific expression patterns. Gene names for transcription factors, ligands, and extracellular matrix molecules are labelled.

c, Human vs. marmoset scatterplots of Am (amnion) vs. PS early (primitive streak early). Highlighted quadrants show human-marmoset conserved markers for each lineage, whereas white quadrants show species-specific expression patterns. Gene names for transcription factors, ligands, and extracellular matrix molecules are labelled.

d, UMAP plots of marmoset CS5-7 or human late CS7 lineages showing normalized log expression of genes highlighted conserved in PS (Primitive streak) early (*WNT8A, SFRP2, MIXL1*) or in Amnion (*GABRP*, *WNT6*, *TFAP2A*)

e, Human vs. marmoset scatterplots of PS (Primitive streak) early vs PS late. Highlighted quadrants show human-marmoset conserved markers for each lineage, whereas white quadrants show species-specific expression patterns. Gene names for transcription factors, ligands, and extracellular matrix molecules are labelled.

f, UMAP plots of marmoset CS5-7 or human late CS7 lineages showing normalized log expression of genes highlighted conserved in PS early (*SOC2, TFAP2C, CDX2*) or in PS late (*SFRP1*, *SHISA*, *SOX2*). Arrows highlight inferred differentiation trajectories of PS early toward mesodermal lineages and PS later toward endodermal lineages.

Supplementary Fig. 12

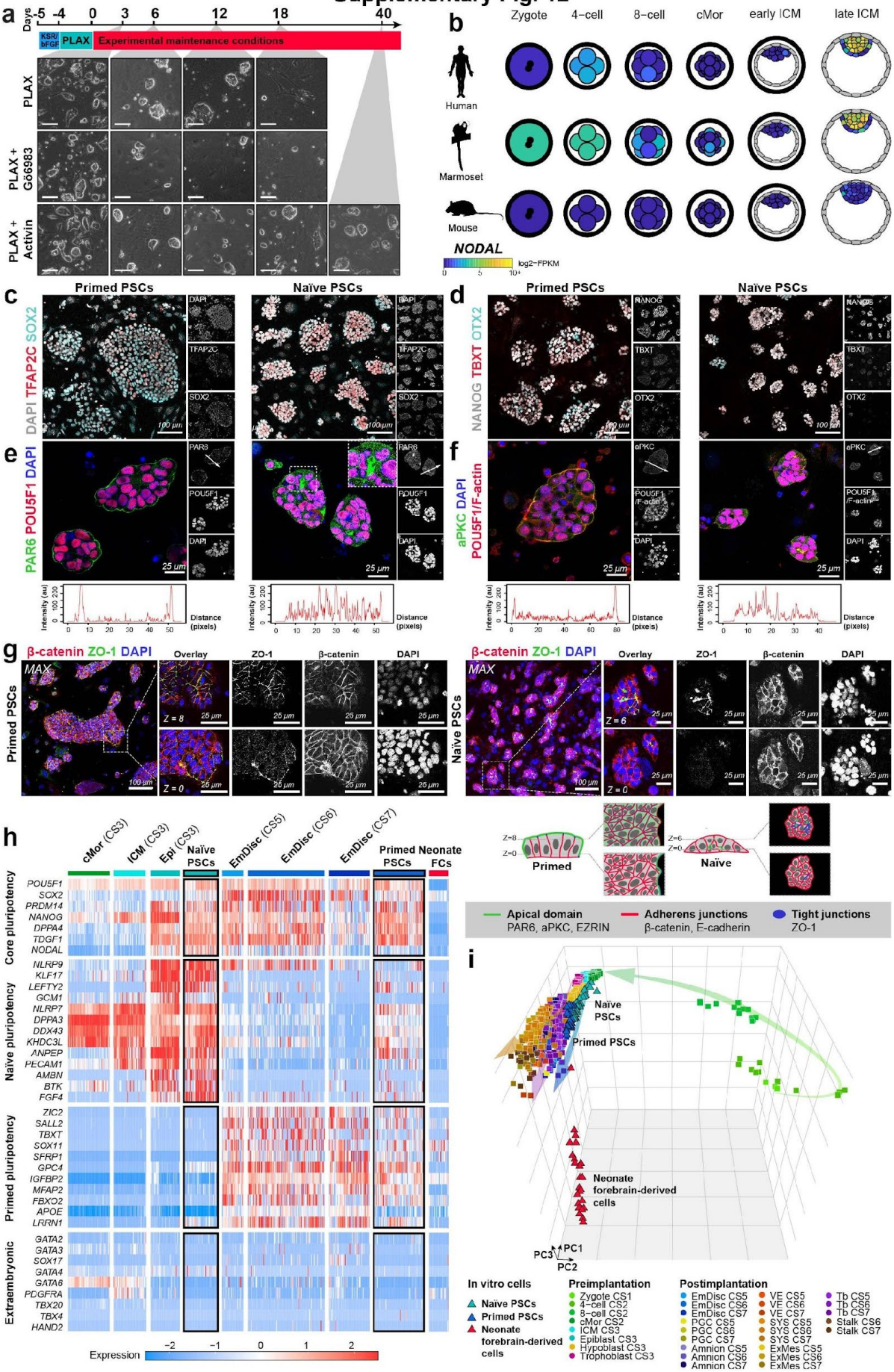

Supplementary Figure 12 | Generation of marmoset naïve pluripotent stem cells.

a, Scheme for resetting marmoset PSCs from primed to naïve pluripotency. Cells were converted by 4-day culture in PLAX (PD03 (1 μM), hLIF (10 ng/mL), AA (50 ng/mL), XAV (5 uM)) and expanded in PLAX, PLAX + Gö6983 (1 μM), or PLAX + human Activin A (20 ng/mL). PLAX + Activin A medium enabled long-term culture; other conditions could not be expanded past day 18-20 (representative of n = 4 independent experiments). Scale bars represent 100μm.

b, *NODAL* expression in human, marmoset and mouse preimplantation embryos, extracted from GRAPPA online database (https://app.stemcells.cam.ac.uk/GRAPPA/)[3].

c-d, Immunostaining of naïve and primed marmoset PSCs for naïve (TFAP2C), primed (TBXT, OTX2) and core (SOX2, NANOG) pluripotency marker genes.

e-f, Representative confocal z-sections of polarity marker immunostaining of naïve and primed marmoset PSCs. White long arrows on PAR6 (e) or aPKC (f) single-channel images indicate the position used to plot intensity profiles (e-f, bottom). Inset is representative of microlumen/rosette formation in naïve PSCs (related to Fig 4a).

g, Maximum intensity projection of polarity marker immunostaining. Representative single-channel images from the top and bottom z-section for each colony at indicated section (z-spacing = 2 μm). Polarity remodelling between naïve and primed PSCs in apical domain, adherens junction, and tight junction localization (in e-g and Fig 4a) summarized in schematic (below).

h, Heatmap of Seurat-normalized gene expression for core pluripotency, naïve and primed pluripotency, and extraembryonic genes extracted from marmoset, human[2] and macaque[1] embryo datasets. Neonate FCs, neonate forebrain-derived cells.

i, PCA of marmoset neonate forebrain-derived cells, *in vitro* cultured PSCs, and embryo samples from zygote to CS7. PCA based on the top 2000 most variable genes, PC1=20.4%, PC2=11.5%, PC3=8.2%.